Desalination and Water Treatment
www.deswater.com

doi: 10.1080/19443994.2015.1137146

57 (2016) 23405–23419
October

Taylor & Francis
Taylor & Francis Group

Simulation of a regeneration plant for spent pickling solutions via spray roasting

D. Bascone[a], A. Cipollina[b], M. Morreale[a,*], S. Randazzo[a], F. Santoro[a], G. Micale[b]

[a]*Facoltà di Ingegneria e Architettura, Università degli Studi di Enna "Kore"—Cittadella Universitaria, 94100 Enna, Italy, email: marco.morreale@unikore.it (M. Morreale)*
[b]*Dipartimento di Ingegneria Chimica, Gestionale, Informatica, Meccanica, Università di Palermo, Viale delle Scienze ed.6, 90128 Palermo, Italy*

Received 9 April 2015; Accepted 24 December 2015

ABSTRACT

Nowadays, pyrohydrolysis techniques are widely applied for regeneration of spent pickling liquors providing an excellent environmental and economical strategy to the problem of waste disposal/recovery, also thanks to the high acid recovery efficiencies (>99%) achieved. In fact, in these processes, iron chlorides are converted into iron oxides and hydrogen chloride at high temperature in spray roasting or fluidized bed reactors. Though the state-of-the-art technologies have been successfully applied only to large-scale plants, the development of small-scale units, able to perform a delocalized regeneration of spent solutions where these latter are actually produced, would be strongly needed in order to minimize the transportation of hazardous spent pickling and fresh HCl solutions to/from pickling factories from/to large centralized regeneration plants. In the present work, a steady-state simulation model for regeneration of spent pickling liquor via spray roasting has been developed, aiming at the analysis of performance of a small-scale unit. The simulation and optimization of the process has been carried out using Aspen Plus simulator. A simplified model of the spray roaster, based on the data collected from studies reported in the literature, has been implemented and exported from Aspen Custom Modeler. Solid recovery from roaster off-gases has been obtained by a cyclone and a Venturi scrubber, where the spent pickling liquor is concentrated prior to be sprayed into the reactor. Hydrogen chloride is absorbed in an adiabatic absorber, where a sub-azeotropic (18–20 wt%) hydrochloric solution is obtained. Prior to the stack, a scrubber is required to wash off the exhaust gases. Several parametric studies have been performed. Different designs of solid separators have been compared in order to investigate the particulate separation efficiency of the process, while absorption column's packing types and rinse water flow rates have been varied in order to investigate their effects on HCl recovery and acid gas emissions.

Keywords: Process simulation; Pyrohydrolysis plant; Hydrochloric acid regeneration

*Corresponding author.

Presented at EuroMed 2015: Desalination for Clean Water and Energy Palermo, Italy, 10–14 May 2015. Organized by the European Desalination Society.

1. Introduction

The pickling process is an essential step in steel production. Since 1950s [1], hydrochloric acid solution has been used to remove oxides scale from the surface. This acid is preferred to sulphuric acid since, although it is more expensive, it leads to higher rate of dissolution and better surface quality [2]. During the pickling treatment ferrous chloride is formed, up to 250 g/L, while the acid concentration decreases by 75–85%. A pickling bath in this condition is considered spent [3], it provides low-rate pickling and hence it needs to be replaced. A sample of spent pickling liquor is shown in Fig. 1, kindly provided by a pickling industry in Sicily.

Nowadays, several techniques exist to regenerate spent pickling liquor, such as membrane or pyrometallurgical techniques [3]. Chloride pyrohydrolysis is a well-established pyrometallurgical process for both the regeneration of spent pickling solutions and the ferric oxide production, according to the following reaction:

$$4FeCl_2(s) + 4H_2O(g) + O_2(g) \rightarrow 8HCl(g) + 2Fe_2O_3(s) - 55\,kJ/mol \quad (1)$$

This reaction can be carried out in spray roasting reactor, the so-called Ruthner technology, or in fluidized bed reactor, the so-called KCH technology [2]. Despite its high operational costs, the pyrometallurgical process presents several advantages even for small plants, specially minimizing the processing time by allowing the solutions to continuously provide the maximum bath activity. Moreover, a basic regeneration facility would involve savings related not only to the purchase of the fresh acid, but also to the transport and disposal of wastes (reducing, consequently, all risks related to their transport). Ferric oxide, also known as haematite, is used in ferrites industry, as a colouring agent in paint and cement industry, to make catalysts and in other applications [2], depending on chemical and physical characteristics [4]. This oxide, initially considered a by-product, clearly represent an important potential profit, for this reason today chloride pyrohydrolysis is also a haematite production process [4]. A world-wide distribution of fluidized beds and spray roasters from 1986 to 1994 reveals that, from small capacity up to 1,000 L/h, spray roasters are largely preferred, maybe because of the high capital costs for the fluidized bed [4]. Furthermore, ferrite industry demands oxides in the form of powder, then preferring spray roasters oxides to fluidized bed granular oxides, although the latters are usually the purest.

The aim of this work is the development of a steady-state simulation model for a small regeneration plant of spent pickling solution via spray roasting. So far, to our best knowledge, no attempt has been done in order to scale down the spray roasting process for operating at small scale in "distributed" regeneration systems, thus minimizing the impact of economic, environmental and social risks related to the transportation of large volumes of spent and fresh pickling solutions between users and large industrial regeneration plants. The present work aims at facing this issue. Aspen Custom Modeler software has been used to implement a simplified model of the spray roaster, while the commercial process simulator Aspen Plus has been used to develop a predictive tool for the design, analysis and optimization of the process.

Fig. 1. Sample of spent pickling liquor.

2. Process description

The spent pickling solution typically consists of 100–130 g/L $FeCl_2$ and 15–70 g/L HCl [4]. This liquor is initially fed to a pre-concentrator unit as a Venturi, where it is concentrated by the hot roaster off-gases. Here, some water and free acid evaporate, but ferrous chloride precipitation must be avoided. This is a key step of the process: the reduction of the spent pickling solution volume allows to size smaller spray roaster (gas velocity inside the reactor must be lower than 1 m/s, in order to reduce entrainment of solid particles in the top gas outlet [5]), heat recovery is achieved, and a second dust separation occurs. In a collecting vessel, vapour and liquid phases are separated and fed, respectively, to the absorber and to the spray roaster.

The geometry of the spray roasting reactor is simple; it is a cylindrical vessel with a conical bottom for the flow of solids to the bottom outlet. Vessels are simply made of mild steel, but a refractory lining is needed. Three or more burners are tangentially placed at the bottom of the cylindrical vessel, in order to set-up a rotational gas flow inside the reactor and, therefore, a good mixing. As fuel, natural gas or LPG are typically used.

The pre-concentrated solution is sprayed under 3–5 atmosphere through several nozzles, usually made of titanium–tantalum or sintered alumina [4], each one with filter insert. The droplets, whose diameter varies from 30 to 600 μm [6] evaporate yielding, after several hydrate forms, the iron oxide particles at 265˚C, when the reaction (1) starts [6,7]. According to Schiemann et al. [6] and Beck et al. [7], the chloride pyrohydrolysis reaction can be described by a two-step mechanism, which total reaction has been previously reported (reaction (1)):

$$4FeCl_2(s) + 4H_2O \rightarrow 8HCl(g) + 4FeO(s) + 508\,kJ/mol \quad (2)$$

$$4FeO(s) + O_2 \rightarrow 2Fe_2O_3(s) - 563\,kJ/mol \quad (3)$$

The bottom outlet of the spray roaster is equipped with a dump valve and a vibrating screen feeder, then a pneumatic conveying system is used to store oxides in storage bins. Since the oxide produced by this technology is a hollow and porous solid (bulk density is approximately 300–500 kg/m^3 [4]), this haematite is a lightweight and easily airborne powder [5], in contrast to the granular oxide product by fluidized bed reactors. The main drawback, compared to the fluidized bed technology, is the lower purity, considering the big difference between the residence time of solids in the two reactors (less than 10 s in spray roasters, hours in fluidized bed [5]). In literature, the value of the typical particle size ranges from 30 to 150 μm [2,5], while value of the specific surface varies from 2.4 to 50 m^2/g [6]. Typical impurities are manganese oxide and, to a lesser extent, oxides of aluminium, chrome, nickel, zinc, silicon, sodium, copper, potassium [1,4]. Ferric oxide market price obviously depends on its chemical and physical properties, and revenue for this sale is one of the most important factors in evaluating process economic, with capital and operating cost [1].

Inside the reactor, large temperature gradients occur: top gas temperature is usually about 400˚C, the average middle temperature is about 650˚C, bottom gas temperature is about 500˚C, while the flame temperature is between 1,250 and 1,700˚C, depending on the oxygen excess [4]. Usually, the gas velocity must be maintained between 0.3 and 1 m/s, in order to minimize the entrainment of the solid phase in the top outlet [5]. For this purpose, spray roaster diameter must be sized large enough, but at the same time it has to lead to high enough velocity to prevent droplets to reach the bottom of the reactor [5]. For the same reason, spray roaster height must be sufficiently high [5]. The hot roaster off gases are sent in one or two cyclones, where usually 15% of particles are recovered, and then are sent in a pre-evaporator system, usually a Venturi, to concentrate the spent pickling solution prior to be fed into the spray roaster. The solids recovered in the cyclone are recycled in the spray roaster. The off-gases, rich in HCl, are sent in an adiabatic packed column, where HCl is absorbed reaching a concentration in the range of 18–20% wt.

Prior to the stack, a scrubber is needed to remove the residual HCl and dust from the off-gases. Besides these pollutants, unwanted combustion products can be present as well, i.e. carbon monoxide and nitrous oxide, while formation of dioxins is never been reported and it is very unlikely [4]. In this tower, a rinse water flow rate is used, and the diluted acid solution produced is used as solvent in the absorber. Usually, for both absorber and scrubber, a polypropylene packing is used. The exhaust gases are sent to the stack and then released to the atmosphere, by an exhaust gas fan made of titanium.

The whole process flow diagram is showed in Fig. 2. This process ensures HCl recovery of 99.9%.

Spent pickling solutions could contain zinc concentration up to 110 g/L [3]. This may be due to several reasons, such as the zinc-covered elements for transportation of the steel from the pickling bath to the galvanizing one, or defectively pickling galvanized steels. Considering the volatility of zinc compounds, zinc concentration higher than 0.5 g/L causes process problems to the spray roaster, i.e. iron oxide contaminations, refractory failure, complete filling of the gas off-take [3,4]. For these reasons, the zinc content must be removed from these liquors prior to be used for the spray roasting plant. This operation can be made by a liquid–liquid extraction plant [8–12].

Because of the combustion reactions, acid gases and particulate production, several air pollutants could be involved in this process. However, hazardous combustion products such as carbon monoxide or nitrous oxides are usually negligible in the exhaust gas that mainly consists in water vapour, nitrogen, oxygen, carbon dioxide and hydrogen chloride. The latter compound and dust represent the main air pollutants to keep under control in the emission, while no presence of dioxins and furans are reported in

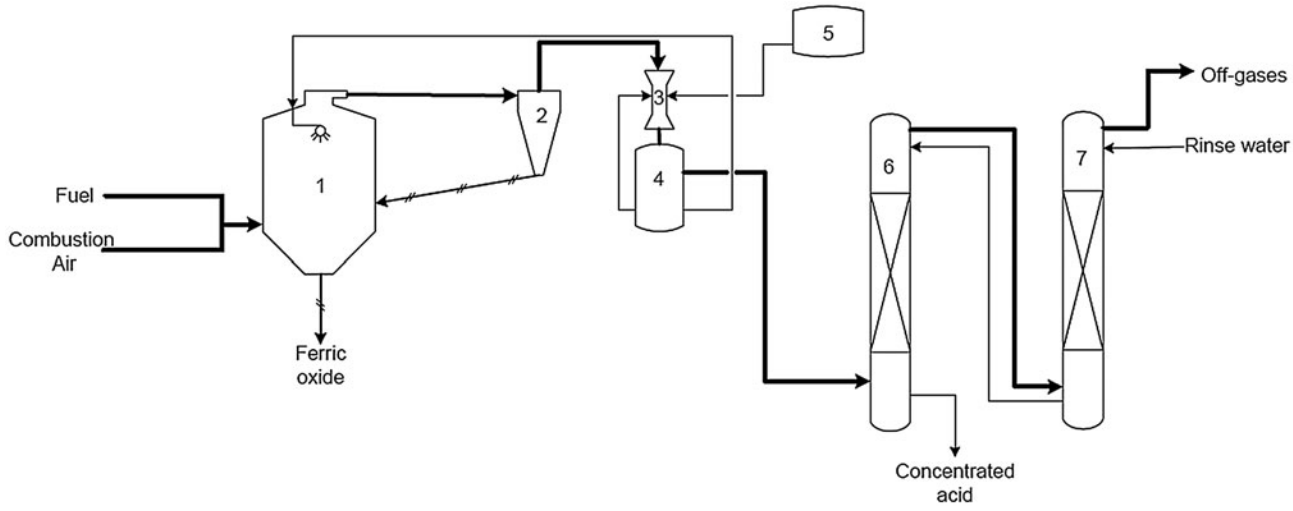

Fig. 2. Typical PFD for a pickling solution regeneration plant via spray roasting.
Notes: 1. Spray roaster, 2. Cyclone, 3. Venturi evaporator, 4. Gas–liquid separator, 5. Spent pickling solution tank, 6. Absorber, 7. Scrubber.

exhaust gases, probably due to the quenching of hot roaster off-gases in the pre-concentrator unit [4]. One of the aims of the simulation tool developed is to predict the emissions and optimize the process in order to maximize HCl recovery maintaining these values under emission limits (i.e. 10 mg/Nm^3 according to the Italian Environmental Code, D.Lgs. 152/06, which follows European Regulations).

3. Modelling of the spray roasting process

In order to simulate the spray roasting process, a model has been developed using Aspen One Engineering tools. A simplified model of the spray roasting reactor has been developed using Aspen Custom Modeler, therefore the whole regeneration plant is implemented through Aspen Plus. In the next paragraphs the model is shown, discussing both the property (i.e. chemical species involved, property method, EOS, equilibrium reaction considered and so on) and the simulation (units and streams description) settings.

3.1. Property settings

All species involved in the simulation must be declared in the property analysis section. Nitrous oxides are considered nitric oxide, iron chlorides are considered in both solution and solid phase. Iron is considered the only metallic species in the spent pickling solution. Components and types used in the simulations are showed in Table A1. Chemistry and some components have been suggested by the Electrolyte Wizard tool. Fifteen reactions are considered, mainly equilibrium reactions, as shown in Table A2.

For the sake of brevity, Tables A1 and A2 are reported in Appendix A.

The physical property method suggested by Aspen Plus for electrolytes has been used, i.e. the electrolyte NRTL model with Redlich–Kwong equation of state.

Since oxide products are hollow spheres with bulk density usually between 300 and 500 kg/m^3, molar volume of solids has been increased approximately by one order of magnitude, in order to adjust the mass density of the particulate and hence make more reliable the solid separators performance (especially the ones based on density difference like cyclone).

Streams class is defined as "MIXCIPSD", i.e. for each stream two substreams are described, the "Mixed" substream (containing liquid and gas phase) and the "CIPSD" substream (solid phase with a particle size distribution).

3.2. Simulation settings

Referring to the process flow diagram shown in Fig. 2, a flowsheet for the plant simulation in Aspen Plus 8.6 has been developed (see Fig. 3), defining the following units:

(1) two mixers;
(2) a spray roaster (ACM model);
(3) a cyclone;
(4) a Venturi scrubber;

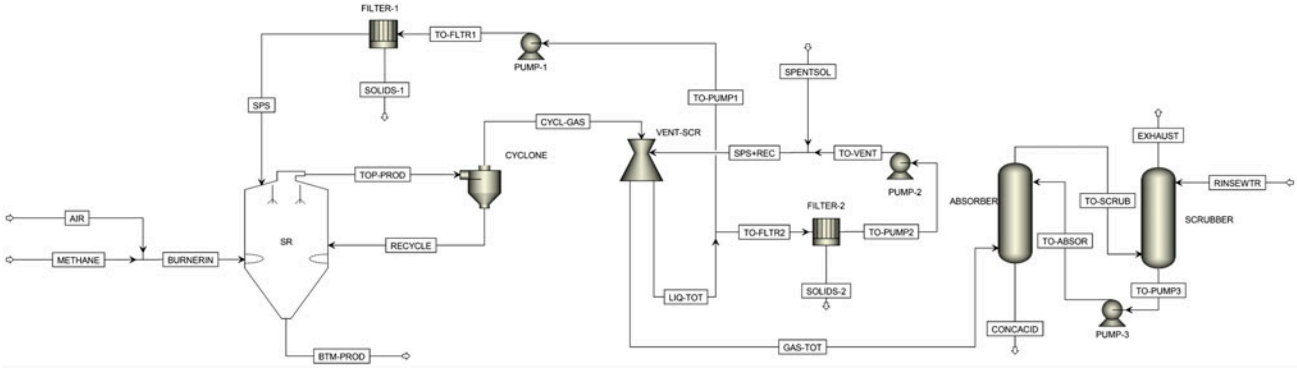

Fig. 3. Flowsheet of the regeneration plant implemented in Aspen Plus 8.6.

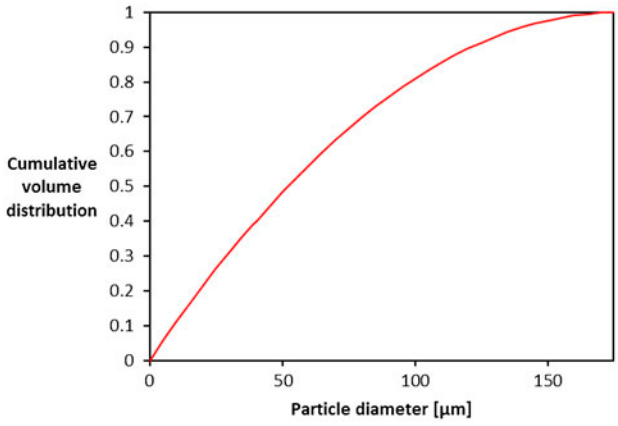

Fig. 4. Particle size distribution used to describe the particle discharge through the top of the reactor.

(5) a splitter;
(6) two substream splitters (filters in Fig. 3);
(7) three pumps;
(8) two absorbtion columns ("RadFrac" columns).

These units will be described in details below.

3.2.1. Spray roaster

For the simulation of the acid regeneration process via spray roasting in Aspen Plus, a unit regarding the spray roaster is needed. For this purpose, a simplified model for this equipment has been modelled by Aspen Custom Modeler, a software for the development of custom models exportable in Aspen Plus flowsheet. The spray roasting reactor has been numerically modelled by diverse authors [13–16], mainly in order to investigate the influence of several geometric parameters, such as nozzle positions. Johansson et al. [16] have performed CFD simulations of the reactor without considering a particle formation model, contrary to Beck et al. [14]. Schiemann et al. [13] have developed a more detailed model, considering boundary diffusion, pore diffusion and chemical kinetics, using kinetic parameters from Vilcu et al. [17] for reaction (2) and from Rollason [18] for reaction (3). They have validated the model by drop tube experiments described in their previous work [6]. Investigating temperature and concentration gradient in the reactor are not the purpose of this work, so the spray roaster has been modelled as a continuous reactor, assuming perfect mixing and temperature homogeneity. Furthermore, gas species are considered ideal gases. Since heat transferred by radiation can be neglected [6], heat balance has been described as a simple enthalpy balance. Values of specific heat capacity and standard enthalpies of formation are taken from literature [19–21], while for ferrous chloride, the value obtained by Cerutti and Hepler is used [22].

According to Beck and Schiemann, chloride pyrohydrolysis reaction has been described by the two steps mechanism, i.e. reactions (2) and (3). Since no laboratory experiments have been carried out in this work, the operating conditions (in terms of average temperature and residence time) and conversion of reactants achieved by Schiemann et al. [13] have been considered, hence the mass balance is expressed as a function of the fractional conversions, where combustion and reactions (2) and (3) are in series (for the sake of brevity, these equations are not reported). Because of the difference of temperature between outlets and average temperature of the reactor, a simple proportion between the typical average temperature and outlet temperatures has been used [4] to calculate the latters. This has been done mainly to adjust the gas outlet temperature, determining for the heat and mass exchange involving this stream in the next units. Particle size distribution has been implemented for solid

products in both outlets, based on the cumulative volume distribution shown by Schiemann et al. and his calculations about the solid entrainment in top outlet [13] (see Fig. 4).

In order to estimate the hazardous combustion products, formation of nitrous oxides and carbon monoxide has been modelled. Three mechanisms are generally accepted for the formation of NO_x: fuel, prompt and thermal NO_x. Natural gas and LPG are used as fuel for spray roasters, and considering that these fuels normally have not organically bound nitrogen, fuel NO_x ought not to be produced by this process. Prompt NO_x, i.e. nitrous oxides formed by reaction between nitrogen, oxygen and hydrocarbon radicals, are usually negligible, compared to the thermal NO_x [23].

The formation of thermal NO_x, oxides produced by the reaction between nitrogen and oxygen at high temperatures, is described by the extended Zeldovich mechanism [24]:

$$N_2 + O \overset{1}{\leftrightarrow} NO + N \tag{4}$$

$$N + O_2 \overset{2}{\leftrightarrow} NO + O \tag{5}$$

$$N + OH \overset{3}{\leftrightarrow} NO + H \tag{6}$$

Rate constants for forward and reverse reactions are [24]:

$$k_{1,\text{for}} = 1.8 \times 10^8 e^{-38.370/T}\ \text{m}^3\,\text{mol}^{-1}\,\text{s}^{-1}$$

$$k_{1,\text{rev}} = 3.8 \times 10^7 e^{-425/T}\ \text{m}^3\,\text{mol}^{-1}\,\text{s}^{-1}$$

$$k_{2,\text{for}} = 1.8 \times 10^4 e^{-4.680/T}\ \text{m}^3\,\text{mol}^{-1}\,\text{s}^{-1}$$

$$k_{2,\text{rev}} = 3.8 \times 10^3 e^{-20.820/T}\ \text{m}^3\,\text{mol}^{-1}\,\text{s}^{-1}$$

$$k_{3,\text{for}} = 7.1 \times 10^7 e^{-450/T}\ \text{m}^3\,\text{mol}^{-1}\,\text{s}^{-1}$$

$$k_{3,\text{rev}} = 1.7 \times 10^8 e^{-24.560/T}\ \text{m}^3\,\text{mol}^{-1}\,\text{s}^{-1}$$

In addition to nitrous oxides, carbon monoxide could be produced during hydrocarbon combustion if mixing of fuel and air, residence time or oxygen excess are not adequate [23]. Because of its relatively high equilibrium concentration at high temperatures, CO concentration could be high even in premixed combustion system [24]. The carbon monoxide oxidation produced by combustion process is due to the reaction involving hydroxyl and hydrogen radicals. Several models and reaction rates have been proposed in literature, but their use requires caution, considering different assumptions and conditions under which they have been developed [24]. As a first approximation, fuel conversion can be assumed unitary and CO produced in burners can be estimated solving equilibrium calculations for the following pool of reactions:

$$CO + OH \leftrightarrow CO_2 + H \tag{7}$$

$$\frac{1}{2}H_2O + \frac{1}{4}O_2 \leftrightarrow OH \tag{8}$$

$$\frac{1}{2}H_2O \leftrightarrow H + \frac{1}{4}O_2 \tag{9}$$

It is worth noting that the estimation of these pollutants, both NO_x and CO, is carried out at the flame temperature.

The mathematical model described above has been implemented in Aspen Custom Modeler, then exported in Aspen Plus. Considering the operating conditions involved in the spray roasting reactor, this unit has been solved using the "Ideal" property method. This method set the ideal gas law as EOS and the activity coefficient for the liquid phase equal to 1. Furthermore, since the mixed substream is a purely gaseous stream, a simplified chemistry (named "C-1") is used, where none of the equilibrium, dissociation or salt reactions occurring in the aqueous phase (see Table A2) are taken into account. Residence time for gaseous products is estimated considering a total volume of the reactor equal to 1 m^3, compatibly with a small-scale plant. Reactor dimensions have been obtained referring to the geometric details provided by Johansson et al. [16]. Reactor sizes are reported in Table 1 (where r_{top} is radius at top, H_{top} height at top, r_{cen} radius at centre, etc.; refer also to Fig. 3 for the reactor shape).

3.2.2. Cyclone

Cyclone unit has been solved in "Simulation" mode. Several equations are available for efficiency calculation and geometry: Sheperd & Lapple equation and Lapple-GP (see Fig. 5) have been used, respectively. The latter has been chosen since the most of the cyclones available in the market seem to present comparable geometry.

Notwithstanding a couple of cyclones are usually employed in the majority of the spray roasting

Table 1
Spray roaster geometry

r_{top} (m)	0.14
H_{top} (m)	0.12
r_{cen} (m)	0.50
H_{cen} (m)	1.02
r_{bot} (m)	0.03
H_{bot} (m)	0.73
r_{spr} (m)	0.17
H_{spr} (m)	0.27
V (m^3)	1
Spray angle (°)	60

regeneration plant, in this work only one cyclone is considered. The Vane constant is set to the default value, i.e. 16. Method and chemistry used are the previous ones employed for the spray roaster.

3.2.3. Venturi scrubber

Two types of Venturi are available in Aspen Plus: one that acts as a simple mixer, and therefore requires a flash drum at a later stage, and another one that acts as a Venturi scrubber, i.e. a Venturi ejector and a liquid–gas drum separator. The latter is commonly used to design the required throat dimension, through several correlations, therefore the Venturi scrubber has been used.

Similarly to the cyclone, this unit has been solved in "Simulation" mode and the throat design is set to "round". In order to calculate the efficiency of the equipment, the Calvert equation has been used. The pressure drop parameter is equal to 0.85, default value, while the grade efficiency parameter is set to 0.5 since this is the suggested value for hydrophilic particulate such as ferric oxide [26,27].

In this unit, differently from the previous one described, mass and energy transfer play a key role, hence from this block chemistry and physical property method described in Section 3.1 must be used.

3.2.4. Absorption columns

In order to simulate the HCl absorption process in absorber and scrubber, two "RadFrac" columns have been employed. These columns are typically used to carry out tray columns simulations, but a packed column can be simulated as well, removing condenser, reboiler and with a null reflux ratio.

The simulation has been performed with "Rate-Based" simulation, and a "Packing Rating" has been defined. Two common types of packing have been used: Berl saddles and Mellapak Plus structured packing, produced by Sulzer. Diameter columns have been estimated considering an 80% flooding, while the packing height have been calculated to obtain outlet HCl concentration lower than the standard value typically accepted for gaseous atmospheric emissions.

3.2.5. Other units

Two mixers are employed. The first one is used to pre-mix fuel and combustion air sent to the spray roaster (67% excess O_2). For computational purpose,

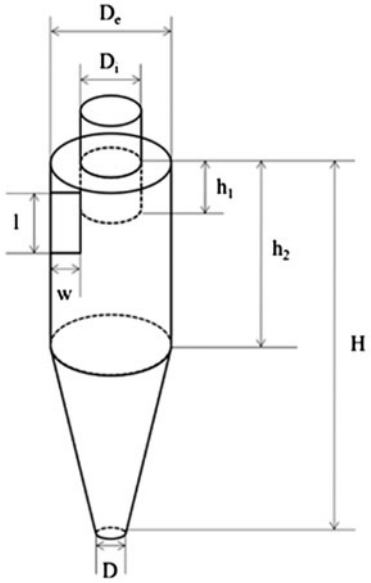

Symbol	Description	Rel. value
	Inlet type: rectangular	
D_e	External diameter	1.0
D_i	Overflow exit diameter (gas outlet)	0.5
h_1	Overflow exit height	0.625
h_2	Cylinder height	2.0
H	Overall height	4.0
D	Bottom diameter (solids outlet)	0.25
l	Gas inlet height	0.5
w	Gas inlet width	0.25

Fig. 5. Geometry of the cyclone with the "Lapple-GP" correlation [25].

this block has been solved using the "Ideal" method and the "C-1" chemistry, similarly to the spray roaster unit. The second mixer is used to mix the spent pickling liquor and the recycled concentrated solution, prior to feed the washing liquid to the Venturi scrubber. This step is essential to achieve a more adequate liquid–gas ratio, in order to increase the separation efficiency of the unit.

A splitter is employed to split into two streams the liquid outlet of the Venturi scrubber. This step is essential to recycle the concentrated solution to the Venturi, in order to achieve an appropriate ratio liquid/gas phase. The split fraction defined is approximately equal to 6%. For flash calculations, only liquid phase is considered.

Two substream splitters have been used as filters, to remove solid suspension (i.e. the CIPSD substream) from liquid streams to be sent into spray nozzles, such as in spray roaster or Venturi scrubber.

Two pumps are employed to raise the pressure of the liquid streams to be sent to spray roaster and Venturi scrubber, while one pump is used to recycle the diluted acid from the scrubber to the absorber.

3.2.6. Streams specifications

Fuel and air are available at 25°C and atmospheric pressure, the excess of oxygen used is 67% [13]. The spent pickling solution has a typical content of HCl and $FeCl_2$, the rinse water is considered pure and available at 25°C and 1 atm, flow rates are variable. Concentrations of the spent pickling solution have been taken from literature [5].

These data are summarized in the Table 2.

4. Parametric analysis of the regeneration plant

A parametric study of the regeneration plant via spray roasting has been performed, in order to investigate the influence of the most important variables on the process performance, i.e. the fuel type, the cyclone and Venturi's geometry, the rinse water flow rate, the HCl concentration in the rinse water, the absorber and scrubber packing height and the packing material, to achieve information about the adequate design of the equipment.

Table 3 shows the details of the studied variables and set conditions, compared with those chosen as reference (entry 1).

For what concern the fuel type, two different fuels have been used, i.e. natural gas (assumed 100% methane) and LPG (assumed 100% propane) (see entry 2).

Parametric analyses of the HCl concentration in the rinse water and its flow rates have been carried out (see Table 3, entries 5, 6), representing a basic and preliminary study for an appropriate design of columns and operating conditions, in order to obtain an enough concentrated hydrochloric solution but, at the same time, a suitable HCl gaseous emission.

Moreover, the influence of the type and the height of the packing have been analysed (see Table 3, entries 7, 8). Two packing materials have been investigated, the Berl saddles and a structured packing.

The obtained main results are summarized in Table 4, at the end of the section.

4.1. Influence of fuel type

Generally, two types of fossil fuels can be used for the regeneration of spent pickling solutions via spray roasting, either natural gas or LPG. In this work, both fuels have been used and results have been compared. Natural gas and LPG are assumed to be, respectively, 100% methane and propane.

For these simulations, the temperature of the spray roaster, the residence time of the gaseous products, the reactor volume and the excess O_2 have been kept constant. Our goal is to observe how the nature of the fuel affects the design and the performance of the equipment in the hot zone of the plant.

As illustrated in Fig. 6, the volume flow rate of the fuel required using natural gas is twice the one required using LPG, since the calorific value of the latter is significantly higher. However, because of the higher O_2/fuel stoichiometric ratio (5, rather than 2), LPG requires a slightly higher air flow rate.

Table 2
Stream conditions defined in this work

Stream	Temperature (°C)	Pressure (atm)	Concentration
Fuel	25	1	100% CH_4 or C_3H_8
Air	25	1	79 v% N_2, 21 v% O_2
Spent pickling solution	25	1	30 g/L HCl, 205 g/L $FeCl_2$
Rinse water	25	1	100% H_2O

Table 3
Summary of the main dependencies investigated in this work

Entry	Investigated variable	Fuel type	Absorber packing height (m)	Scrubber packing height (m)	Packing material	Rinse water flow rate (L/h)	HCl conc. in rinse water (g/L)
1	Reference conditions	Natural gas	10	10	Berl saddles	22	0
2	Fuel	Natural gas or LPG	10	10	Berl saddles	22	0
3	Cyclone geometry	Natural gas	10	10	Berl saddles	22	0
4	Venturi geometry	Natural gas	10	10	Berl saddles	22	0
5	Rinse water flow rate	Natural gas	10	10	Berl saddles	10–50	0
6	HCl concentration in rinse water	Natural gas	10	10	Berl saddles	22	0–20
7	Packing height	Natural gas	5–15	5–15	Berl saddles	22	0
8	Packing type	Natural gas	1–10	1	Berl saddles or Mellapak Plus	22	0

Table 4
Summary of the main results

Investigated variable	Investigated conditions	Optimal condition
Fuel	Natural gas or LPG	Natural gas
Cyclone geometry	Eff. 80% and ΔP 2 kPa	Diameter 12 cm
Venturi geometry	Eff. 80% and ΔP 11 kPa	Throat diameter 2.5 cm
Rinse water flow rate	10–50 (L/h)	22 (L/h)
HCl concentration in rinse water	0–20 (g/L)	0 (g/L)
Packing height	5–15 m (with Berl saddles)	10 m
Packing type	Berl saddles or Mellapak Plus	Mellapak Plus

Furthermore, a higher volume of gaseous product has been observed using LPG, especially regarding carbon dioxide (see Fig. 7). Consequently, also the estimated concentration of the carbon monoxide increase, approximately by 170% (Fig. 8). Besides, NO_x increased as well, because of the higher amount of nitrogen in the chamber, anyway this product is negligible and two order of magnitude lower than the limit values.

The main drawback of the LPG seems to be related to the higher volume of gases involved in the spray roaster, operating with the same excess O_2 and temperatures. Assuming the same time residences and equal reactor volume, this condition leads to lower flow rates of spent pickling solution to be fed, approximately by 20%, as shown in Fig. 8.

4.2. Influence of the cyclone geometry

In a process simulator like Aspen Plus, to design a cyclone only the diameter is needed to be specified,

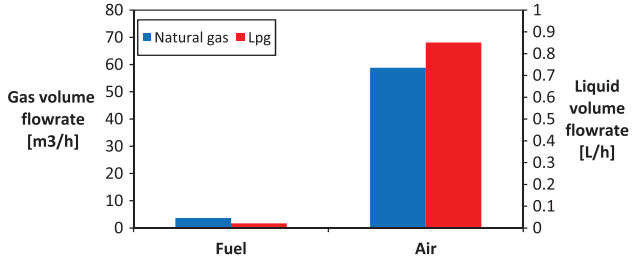

Fig. 6. Influence of the fuel on the volume flow rate of gaseous streams required and of the spent pickling solution stream to regenerate.

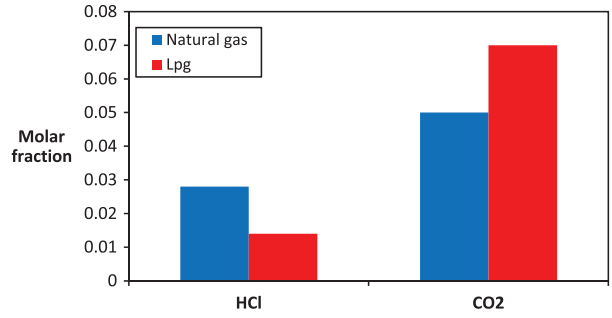

Fig. 7. Influence of the fuel on the concentration, in terms of molar fractions of hydrogen chloride and carbon dioxide in the gaseous product of the spray roasting reactor.

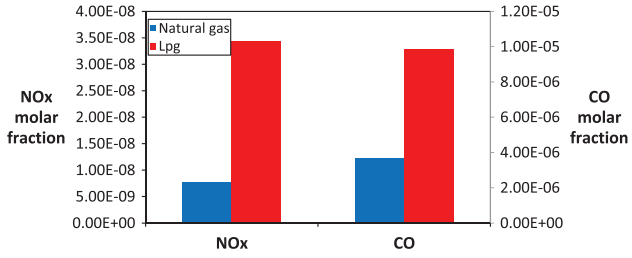

Fig. 8. Influence of the fuel on the concentration, in terms of molar fractions, of nitrous oxide and carbon monoxide in the gaseous product of the spray roasting reactor.

then the geometry has been calculated according to the Lapple-GP geometry proportions. The influence of the diameter on the cyclone performance has been investigated, in order to find the most appropriate condition in terms of supportable pressure drop and solid separation efficiency.

As shown in Fig. 9, a compromise between separation efficiency and pressure drop must be found, since the smaller is the cyclone the higher is the gas velocity and then both pressure drop and solid recovery. In literature, a pressure drop of 2 kPa is reported [5], so the solid separation efficiency in this condition would be about 80%. This is a realistic value, in relation to the particle size distribution defined in this work.

4.3. Influence of the Venturi geometry

The Venturi ejector acts as successive step for the separation of the particulate matter not recovered by the cyclone. In this equipment the smaller particulate is involved, approximately with diameter lower than 10 μm. In Aspen Plus, similarly to the cyclone, the parameter to design the Venturi ejector related to the separation efficiency is the throat size. Both the throat's diameter and length can be designed, but for reasons of calculations simplicity the latter has not been considered.

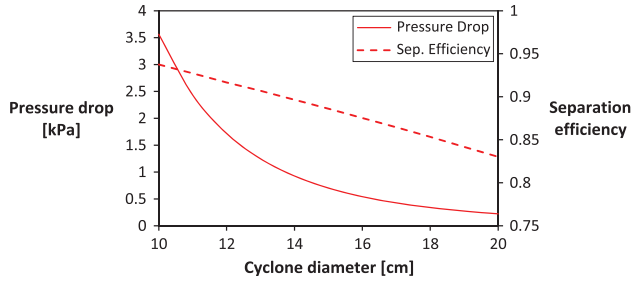

Fig. 9. Influence of the cyclone diameter on the separation efficiency and the pressure drop.

The influence of the throat diameter on the Venturi efficiency and pressure drop has been investigated (see Fig. 10). As expected, the throat diameter clearly affects the gases velocity into the throat, where the atomized liquid separates the solid particulate, and consequently the separation efficiency: the smaller is the diameter, the higher is the separation efficiency. Because of higher gases velocity, the pressure drop is higher. According to Adham et al. [5], an assumable value for the pressure drop is 11 kPa, then the throat diameter should be approximately 2.5 cm, with solid separation efficiency equals to about 80%.

4.4. Influence of the rinse water flow rate

The effect of the rinse water flow rate on the absorption process has been investigated. For these simulations, Berl saddles (ceramic, 6 mm) have been used as packing and the packing height of both absorber and scrubber has been set to 10 m.

As shown in Fig. 11, the rinse water flow rate strongly affects the HCl concentration in the regenerated acid solution: the higher is the flow rate, the more diluted is the acid solution. The highest HCl concentration, of 20% w/w HCl, close to the azeotropic composition, is achieved with a flow rate between 10 and 15 L/h. However, employing only one scrubber column, these operating conditions may not be appropriate, since exhaust off-gases concentrations could be conflicting with the emission limit values. However, a good compromise is achieved setting a 22 L/h flow rate.

Fig. 12 illustrates the influence of the rinse water flow rate on the HCl % recovery of the process. As expected, the HCl recovery shows an upward trend, but then level off. The initial increase is due to the higher amount of solvent available for the HCl absorption, but for values higher than 20 L/h the HCl recovery is practically complete, therefore the water flow rate does not affect it anymore.

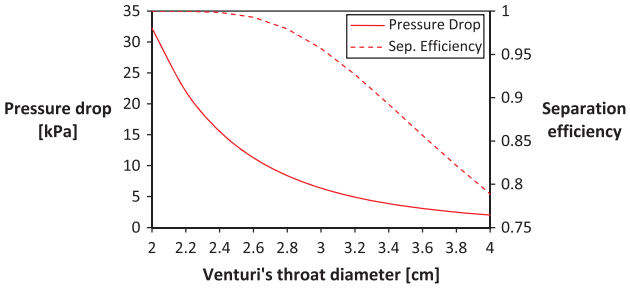

Fig. 10. Influence of the Venturi's throat diameter on the separation efficiency and the pressure drop.

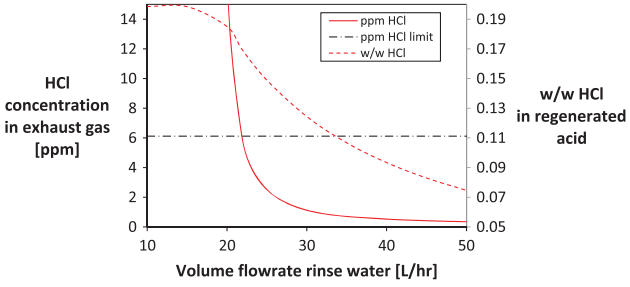

Fig. 11. Influence of rinse water flow rate on the HCl concentration in the regenerated acid solution and in the atmospheric emission.
Notes: Packing height of both absorber and scrubber is 10 m, packing type is Berl saddles. Rinse water concentration: pure water. Fuel: natural gas.

4.5. Influence of HCl concentration on rinse water

Since the rinse water comes from the galvanizing plant, it inevitably is a diluted hydrochloric acid solution, and using demineralized water would not be economical. The influence of the free acid content in this stream on the products of the process has been investigated and results are shown in Fig. 13. The higher is the HCl concentration in the rinse water stream, the higher is the acid concentration in the regenerated solution, the upward trend is quite linear.

On the other hand, higher free acid concentration of the rinse water solution leads to a higher HCl concentration in the exhaust gases. This value must be accurately observed, since it can easily exceed the limit value. As shown in Fig. 13, there is a remarkable difference between a pure water and a very diluted hydrochloric acid solution such as 20 g/L (i.e. less than 0.02% w/w): for the first one, the standard emission of hydrogen chloride is not exceeded, for the second one the HCl emission is almost one order of magnitude higher than the limit values, therefore this condition would require higher packing heights or water flow rates.

Fig. 14 depicts the influence of the HCl concentration on the rinse water flow rate in the HCl recovery of the regeneration facility. Since the operating conditions simulated provide an almost complete HCl recovery, a significant effect of the HCl concentration in the rinse water on this variable is practically not observed. Although the increase in the HCl concentration in the rinse water should, theoretically, reduce the driving force for the HCl mass transfer, a reduction on the HCl is negligible, because of the low range of HCl concentration in the rinse water analysed.

4.6. Influence of packing height

The influence of the packing height is analysed in this paragraph. The monitored variables, as in the previous paragraphs, are the HCl composition in both acid solution and exhaust gases, and the HCl recovery. In these simulations, same packing heights have been used for both absorber and scrubber column.

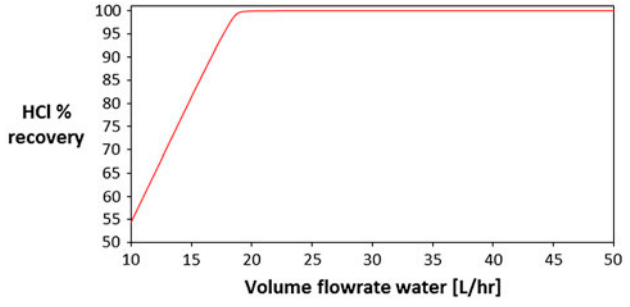

Fig. 12. Influence of rinse water flow rate on the HCl % recovery of the regeneration plant.
Notes: Packing height of both absorber and scrubber is 10 m, packing type is Berl saddles. Fuel: natural gas.

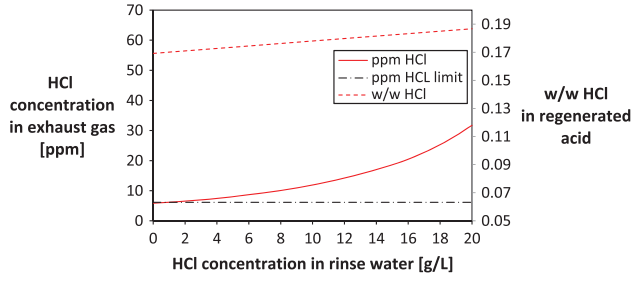

Fig. 13. Influence of the HCl concentration on the rinse water flow rate on the HCl concentration in the regenerated acid solution and in the atmospheric emission.
Notes: Packing height of both absorber and scrubber is 10 m, packing type is Berl saddles. Rinse water flow rate 22 L/h. Fuel: natural gas.

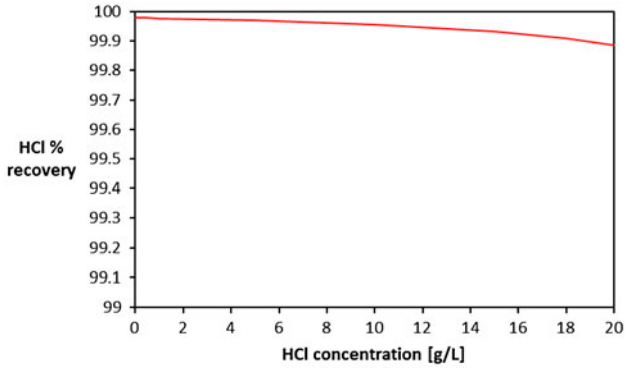

Fig. 14. Influence of the HCl concentration on the rinse water flow rate on the HCl recovery of the plant.
Notes: Packing height of both absorber and scrubber is 10 m, packing type is Berl saddles. Rinse water flow rate 22 L/h. Fuel: natural gas.

Considering the high solubility of hydrogen chloride in aqueous solution, the packing height seems to not significantly affect the HCl concentration in the regenerated pickling solution, because it is fairly close to the equilibrium concentration up to low packing heights (see Fig. 15). On the contrary, the packing height markedly affects the acid content in the exhausted gases. The reason is due to the small scale of interest: being the permitted HCl concentration in the atmospheric emission in the order of ppm, even little changes in the packing height lead to significant variation in the HCl concentration in the off-gases, so the packing height plays a determining role in the outlet concentration. As shown in the Fig. 15, the acceptable packing height, in order to meet the emission requirements, has to be higher than 10 m.

As shown in Fig. 16, higher packing heights leads to higher HCl recovery. Anyway, depending the HCl recovery mainly on the water flow rate used, in the condition simulated the HCl recovery is almost 100%, than the packing height slightly affects the HCl recovery.

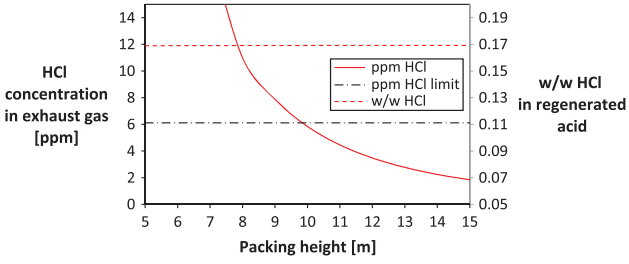

Fig. 15. Influence of packing height of absorber and scrubber on the HCl concentration in the regenerated acid solution and in the atmospheric emission.
Notes: Rinse water flow rate 22 L/h, packing type is Berl saddles. Rinse water concentration: pure water. Fuel: natural gas.

4.7. Influence of packing material

In order to evaluate the influence of the packing type on the columns performance, simulations have been performed using two different packings: Berl saddles, a typical and well-known packing type, and a structured packing produced by Sulzer, the Mellapak Plus 252.Y, widely employed for acid gas absorption. Berl saddles used are manufactured by a generic vendor, in ceramic material and with the dimension set to 6 mm. Both packings were already defined in the Aspen Plus libraries.

As expected, the higher specific area of the structured packing leads to lower packing height. The results obtained using a 10-m Berl saddles packing height have been reproduced using a 5.8 m structured packing height, hence of the Mellapak Plus entails a 42% reduction of the packing height. The performances of the two packing geometry are compared in Fig. 17: the Mellapak Plus packing leads to lower HCl emission and slightly more concentrated hydrochloric solution, i.e. to higher HCl recovery (see Fig. 18). These trends are due to the higher surface area available for the gas–liquid interface provided by the structured packing.

In order to enhance the different behaviour of the two packing types, the packing height of the scrubber column in these simulations is set to 1 m: the performance of the two different packing types would have not otherwise been noticeable, because of the practically complete HCl recovery achieved using higher scrubber packing height.

As observable, the advantages of the structured packing on the HCl recovery are particularly marked

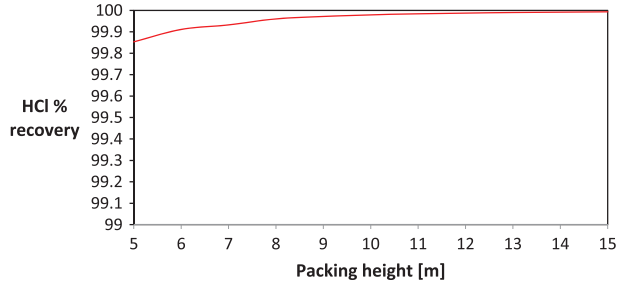

Fig. 16. Influence of packing height of absorber and scrubber on the HCl % recovery of the regeneration plant.
Notes: Rinse water flow rate 22 L/h, packing type is Berl saddles. Rinse water concentration: pure water. Fuel: natural gas.

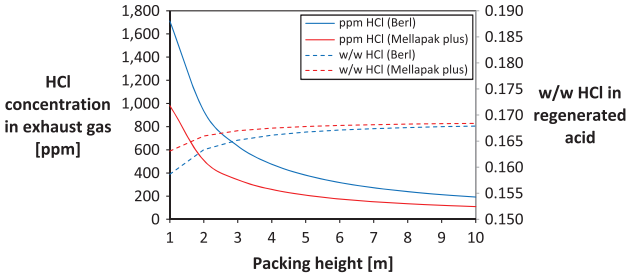

Fig. 17. Influence of the packing type on the HCl concentration in the regenerated acid solution and in the atmospheric emission vs. packing height of the absorber.
Notes: Scrubber packing height is equal to 1 m. Rinse water flow rate 22 L/h. Rinse water concentration: pure water. Fuel: natural gas.

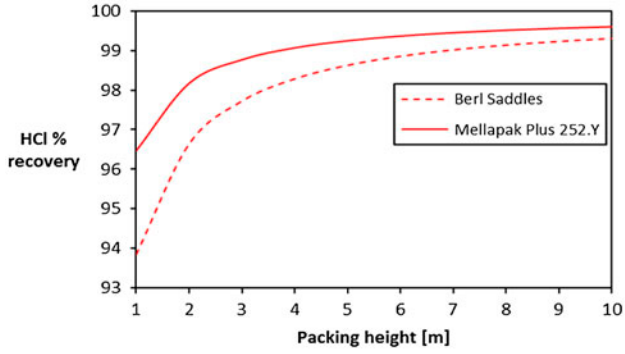

Fig. 18. Influence of the packing type on the HCl recovery of the plant vs. packing height of the absorber.
Notes: Scrubber packing height is equal to 1 m. Rinse water flow rate 22 L/h. Rinse water concentration: pure water. Fuel: natural gas.

at low packing height, where there still is a little but significant difference between the amounts of absorbed HCl and the equilibrium values, while at higher packing height both packing types are fairly close to 100% acid recovery and the higher surface area is not exploited.

Main results obtained in this parametric analysis of the regeneration plant are summarized in Table 4.

5. Conclusions

A modelling tool has been developed to simulate the regeneration process of spent pickling solutions through spray roasting technology. Future developments of this work would obviously include the use of the information coming from simulations for the design of a small-scale prototype.

The regeneration plant mainly involves a spray roasting reactor, a cyclone, a Venturi scrubber and two packed column (absorber and scrubber). The Aspen Plus process simulator has been used to design and optimize the process. A simplified model of the spray roasting reactor, i.e. a steady-state conversion reactor, has been developed using Aspen Custom Modeler. The influence of several parameters has been investigated: fuel type (i.e. natural gas or LPG), cyclone geometry, Venturi geometry, rinse water flow rate, HCl concentration in the rinse water, packing heights, packing material.

For the first parametric study, gaseous pyrohydrolysis products (pollutants included) and the effect of the gaseous streams required on the reactor size have been analysed. Regarding the simulations involved the solid separators, separation efficiency and pressure drop have been studied. Finally, for the other parametric studies, HCl concentrations in both regenerated hydrochloric solution and exhaust gas have been monitored, as well as the HCl recovery of the whole regeneration plant. Average temperature reactor and O_2 excess being equal, the choice of the natural gas as fuel seems to be more appropriate. This fuel involves less gaseous volume in the reactor, in terms of both gaseous product and combustion air required, even though the fuel stream required is higher than the LPG stream (because of the lower methane's heating value). Furthermore, the natural gas leads to lower CO_2, CO and NO_x emissions. Lower cyclone's diameter positively affects the solid recovery, since higher gas velocities are involved. However, the pressure drop increases thus a compromise between these two variables must be found. Similar considerations can be made for the Venturi's throat diameter. Common pressure drop reported for cyclone and Venturi separator are, respectively, 2 and 11 kPa. At these conditions, separation efficiency of approximately 80% is achieved for both units. Rinse water flow rate dramatically affects the performance of the regeneration plant, in terms of HCl concentrations in the outlet streams (regenerated acid and exhaust gas), and therefore in terms of HCl recovery. Since higher flow rates lead to higher HCl recovery but lower HCl concentrations in the regenerated pickling solution, a rinse water flow rate of 22 L/h has been selected in order to achieve HCl recovery higher than 99%. Regarding the influence of HCl concentration on the rinse water, the results of the simulations show that the presence of HCl in the rinse water may easily lead to excessive HCl content in the exhaust gas. Hence, the higher is the HCl concentration in the rinse water flow rate, the higher must be the rinse water flow rate or the column's packing height. Packing heights of both columns significantly affect the HCl concentrations in the exhaust gas. Because of the limit values permitted for

atmospheric gaseous emissions, HCl concentrations in this stream must be lower than 6 ppm. This value lead to packing height of 10 m for both columns, considering ceramic Berl saddles as packing. The influence of two different packing materials has been investigated, i.e. Berl saddles and a structured packing, Sulzer Mellapak Plus 252.Y. As expected, the higher surface area of the latter lead to better performance of the absorption columns, allowing to significant reduction of the packing height.

Acknowledgements

The authors acknowledge the financial support from the Italian Research Project "PO FESR Sicily 2007–2013 – Measure 4.1.1.1 – Green Waste – CUP G23F12000050004" funded through the Sicilian Regional Government and the European Union.

References

[1] M. Ruthner, O. Ruthner, 25 Years of process development in HCl pickling and acid regeneration, Iron Steel Eng. 56(11) (1979) 36–39.
[2] W.F. Kladnig, New development of acid regeneration in steel pickling plants, J. Iron Steel Res., Int. 15(4) (2008) 1–6.
[3] M. Regel-Rosocka, A review on methods of regeneration of spent pickling solutions from steel processing, J. Hazard. Mater. 177 (2010) 57–69.
[4] E.M.L. Peek, Chloride Pyrohydrolysis—Lixiviant Regeneration and Metal Separation, Delft University Press, Delft, 1995, pp. 57–77.
[5] K. Adham, C. Lee, D. Small, Energy consumption for iron chloride pyrohydrolysis: A comparison between fluidized beds and spray roasters, in: J.E. Dutrizac, P.A. Riveros (Eds.), Iron Control Technol., Montreal, 2006, pp. 815–829.
[6] M. Schiemann, S. Wirtz, V. Scherer, F. Bärhold, Spray roasting of iron chloride $FeCl_2$: Laboratory scale experiments and a model for numerical simulation, Powder Technol. 228 (2012) 301–308.
[7] M. Beck, S. Wirtz, V. Scherer, Experimental and numerical studies of Fe_2O_3 particle formation processes in a flat flame burner, Chem. Eng. Technol. 30 (2007) 790–796.
[8] T.H. Tuneley, P. Kohler, T.D. Sampson, The Metsep process for the separation and recovery of zinc, iron and hydrochloric acid from spent pickle liquors, J. S. Afr. Inst. Min. Metall. 76 (1976) 423–472.
[9] M.B. Mansur, S.D. Ferreira Rocha, F.S. Magalhaes, J. dos Santos Benedetto, Selective extraction of zinc(II) over iron(II) from spent hydrochloric acid pickling effluents by liquid–liquid extraction, J. Hazard. Mater. 150 (2008) 669–678.
[10] K. Sarangi, P.K. Parhi, E. Padhan, A.K. Palai, K.C. Nathsarma, K.H. Park, Separation of iron(III), copper (II) and zinc(II) from a mixed sulphate/chloride solution using TBP, LIX 84I and Cyanex 923, Sep. Purif. Technol. 55 (2007) 44–49.
[11] S.I. El Dessouky, Y.A. El-Nadi, I.M. Ahmed, E.A. Saad, J.A. Daoud, Solvent extraction separation of Zn (II), Fe(II), Fe(III) and Cd(II) using tributylphosphate and CYANEX 921 in kerosene from chloride medium, Chem. Eng. Process. 47 (2008) 177–183.
[12] S. Randazzo, D. Bascone, V. Caruso, M. Morreale, G. Micale, A. Cipollina, Recovering of zinc(II) from spent pickling solutions by liquid–liquid extraction, EuroMed Conference Proceedings, 10–14 Maggio 2015, Palermo, Italy.
[13] M. Schiemann, S. Wirtz, V. Scherer, F. Bärhold, Spray roasting of iron chloride FeCl2: Numerical modelling of industrial scale reactors, Powder Technol. 245 (2013) 70–79.
[14] M. Beck, S. Wirtz, V. Scherer, F. Bärhold, Numerical calculations of spray roasting reactors of the steel industry with special emphasis on Fe_2O_3-particle formation, Chem. Eng. Technol. 30 (2007) 1347–1354.
[15] L. Westerberg, V. Geza, A. Jakovics, Burner backflow reduction in regeneration furnace, Eng. App. Comput. Fluid Mech. 5 (2010) 372–383.
[16] S. Johansson, V. Geza, L.G. Westerberg, A. Jakovics, Characteristics of flow and temperature distribution in a Ruthner process, 6th International Scientific Colloquium: Modelling for Material Processing, University of Latvia, Riga, 2010, pp. 317–322.
[17] R. Vilcu, T. Coseac, D. Oancea, Some kinetic aspects of the high-temperature anhydrous $FeCl_2$ hydrolysis reaction, Rev. Roum. Chim. 42 (1997) 93–97.
[18] R.J. Rollason, J.M.C. Plane, The reactions of FeO with O_3, H_2, H_2O, O_2 and CO_2, Phys. Chem. Chem. Phys. 2 (2000) 2335–2343.
[19] R.C. Perry, D.W. Green, Perry's Chemical Engineers' Handbook, seventh ed., McGraw-Hill, New York, NY, 1999.
[20] R.K. Sinnott, Coulson & Richardson's Chemical Engineering, Chemical Engineering Design, vol. 6, fourth ed., Elsevier Butterworth-Heinemann, Oxford, 2005.
[21] P. Patnaik, Handbook of Inorganic Chemicals, McGraw-Hil, New York, NY, 2003.
[22] P.J. Cerutti, L.G. Hepler, The enthalpy of solution of ferrous chloride in water at 298 K, Thermochim. Acta 20(3) (1997) 309–314.
[23] I.V. Ion, F. Popescu, L. Georgescu, Prediction of the pollutants generation in natural gas/residual steel gases co-combustion, Int. J. Energ. Environ. 1(2) (2007) 79–84.
[24] R.C. Flagan, J.H. Seinfeld, Fundamentals of Air Pollution Engineering, Prentice Hall, Englewood Cliffs, New Jersey, 1988.
[25] C.B. Shephered, C.E. Lapple, Flow pattern and pressure drop in cyclone dust collectors, Ind. Eng. Chem. 31 (1939) 972–984.
[26] Y. Koide, K. Esumi, Physicochemical properties of ring-structured surfactants, in: K. Esumi, M. Ueno, (Eds.), Structure-Performance Relationships in Surfactants, second ed., Marcel Dekker Press, New York, NY, 2003, pp. 320–351 (Chapter 6).
[27] D. Szyszka, Study of contact angle of liquid on solid surface and solid on liquid surface, Prace Nauk. Inst. Gorn., Politech. Wrocławskiej 135 (2012) 131–146.

Appendix A

Table A1
List of species used in this work

Component ID	Type
C_3H_8	Conventional
CH_4	Conventional
Cl^-	Conventional
CO	Conventional
CO_2	Conventional
CO_3^-	Conventional
$Fe(OH_3^-)$	Conventional
Fe^{++}	Conventional
$Fe(OH_3^-)$	Conventional
Fe_2O_3	Solid
$Fe(OH)_2$	Solid
$FeCl_2{\cdot}4H_2O$	Solid
$FeCl_2{\cdot}2H_2O$	Solid
$FeCl_2$	Conventional
$FeCl_2$(S)	Solid
FeO	Solid
$FeOH^+$	Conventional
H^+	Conventional
H_2O	Conventional
HCl	Conventional
HCO_3^-	Conventional
N_2	Conventional
NO	Conventional
O_2	Conventional
OH^-	Conventional

Table A2
List of reactions defined in the chemistry section

Equilibrium	$3\ OH^- + Fe^{++} \leftrightarrow Fe(OH_3^-)$
Equilibrium	$FeOH^+ \leftrightarrow Fe^{++} + OH^-$
Equilibrium	$HCl \leftrightarrow Cl^- + H^+$
Equilibrium	$HCO_3^- \leftrightarrow CO_3^- + H^+$
Equilibrium	$H_2O + CO_2 \leftrightarrow HCO_3^- + H^+$
Equilibrium	$H_2O \leftrightarrow OH^- + H^+$
Salt	$FeCl_2{\cdot}2H_2O \leftrightarrow Fe^{++} + 2\ H_2O + 2\ Cl^-$
Salt	$FeCl_2{\cdot}4H_2O \leftrightarrow Fe^{++} + 2\ Cl^- + 4\ H_2O$
Salt	$FeCl_2$(S) $\leftrightarrow Fe^{++} + 2\ Cl^-$
Salt	$Fe(OH)_2 \leftrightarrow FeOH^+ + OH^-$
Dissociation	$FeCl_2 \leftrightarrow Fe^{++} + 2\ Cl^-$